

Origin of spin-glass behavior of $\text{Zn}_{1-x}\text{Mn}_x\text{O}$

S. Kolesnik, B. Dabrowski, and J. Mais

Department of Physics, Northern Illinois University, DeKalb, IL 60115

(Dated: November 13, 2018)

ac susceptibility has been studied for polycrystalline $\text{Zn}_{1-x}\text{Mn}_x\text{O}$. Stoichiometric samples demonstrate Curie-Weiss behavior, which indicates mostly antiferromagnetic interactions. Magnetic susceptibility can be described by a diluted Heisenberg magnet model developed for semimagnetic semiconductors. High-pressure oxygen annealing induces spin-glass like behavior in $\text{Zn}_{1-x}\text{Mn}_x\text{O}$ by precipitation of ZnMnO_3 in the paramagnetic matrix.

Keywords: Diluted magnetic semiconductor, $\text{Zn}_{1-x}\text{Mn}_x\text{O}$, synthesis, spin-glass behavior

The incorporation of spin into semiconductor electronics requires fabrication of ferromagnetic semiconductors with the Curie temperature higher than room temperature. Theoretical predictions of room temperature ferromagnetism in diluted magnetic semiconductors [1] recently brought wide attention to this class of materials. According to these calculations, *p*-type $\text{Zn}_{1-x}\text{Mn}_x\text{O}$ is a promising candidate for a room temperature ferromagnet. Ab initio band calculations [2] predict ferromagnetism to be stable in *p*-type $\text{Zn}_{1-x}\text{Mn}_x\text{O}$, and antiferromagnetism in *n*-type $\text{Zn}_{1-x}\text{Mn}_x\text{O}$. On the other hand, a ferromagnetic phase has been predicted for *n*-type ZnO substituted with Fe, Co, or Ni. [3] Various substitutions (B, Al, Ga, In, Si, and F) in the parent compound ZnO can increase its natural *n*-type conduction, caused by oxygen vacancies and Zn interstitials. [4] However, only a few attempts to introduce *p*-type conduction into ZnO have been so far successful. This includes nitrogen doping [4] and, the theoretically proposed [5] Ga and N codoping. [6] Preparation of *p*-type ZnO could find application in optoelectronic devices (e. g. solar cells, short-wavelength light emitting diodes) and also allow fabrication of transparent *p* - *n* junctions.

Pulsed-laser deposited $\text{Zn}_{1-x}\text{Mn}_x\text{O}$ thin films without intentional carrier doping show spin-glass behavior. [7] According to this study, Mn can be dissolved in the ZnO matrix to over 35%. ZnO films doped with other transition metals (Co, Cr, Ni) have been reported to be ferromagnetic in case of Co doping. [8] Ferromagnetism, however, was observed for only 10% of studied thin films. Magnetic properties of bulk $\text{Zn}_{1-x}\text{Mn}_x\text{O}$ have not yet been reported.

In this study we investigate polycrystalline $\text{Zn}_{1-x}\text{Mn}_x\text{O}$ ($x = 0.05 - 0.20$). The studied samples were prepared in air at $T = 1350^\circ\text{C}$ using a standard solid-state reaction technique. The samples were then annealed in an atmosphere of different gases (Ar, H_2 , as well as O_2 under high pressure of 600 bar). ac susceptibility and dc magnetization were measured using a Physical Property Measurement System (Quantum Design). X-ray diffraction spectra have been collected using a Rigaku X-ray diffractometer. The samples are mostly dark green. Annealing in a reducing H_2 atmosphere changes their color to orange or brown,

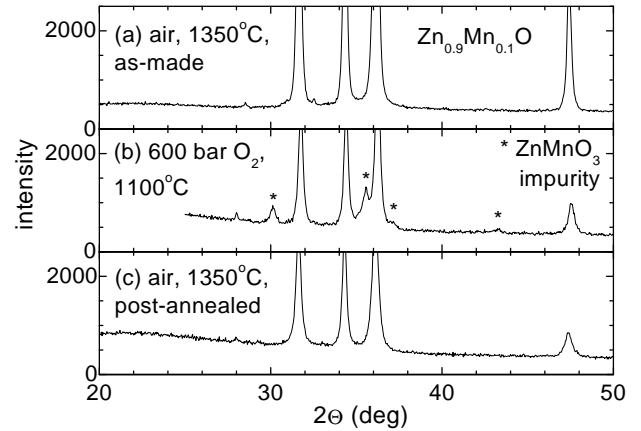


FIG. 1: X-ray diffraction patterns for $\text{Zn}_{0.9}\text{Mn}_{0.1}\text{O}$ samples synthesized in air (a), high-pressure oxygen-annealed (b), and subsequently annealed in air (c).

which points at the decrease of the energy gap below the value of 3.2 eV characteristic for ZnO. X-ray diffraction data show that the $x \leq 0.1$ samples annealed in air are single-phase with the wurtzite structure as of ZnO. $\text{Zn}_{1-x}\text{Mn}_x\text{O}$ with $x = 0.15$ and 0.2 show small amount of spinel-like ZnMn_2O_4 . This observation suggests that the solubility limit in air is reached near $x = 0.1$, significantly lower than reported for $\text{Zn}_{1-x}\text{Mn}_x\text{O}$ thin films. [7] High-pressure oxygen annealing causes appearance of the ZnMnO_3 second phase that can be removed by subsequent annealing in air. Fig. 1 shows X-ray diffraction patterns for the $\text{Zn}_{0.9}\text{Mn}_{0.1}\text{O}$ sample for such a sequence of annealings. We observe the presence of impurity peaks for the high-pressure annealed sample.

Magnetic susceptibility for $\text{Zn}_{1-x}\text{Mn}_x\text{O}$ is presented in Fig. 2. ac susceptibility of the Mn-doped ZnO at temperatures $T = 120 - 350$ K resembles Curie-Weiss behavior that is also characteristic for other Mn-containing semimagnetic semiconductors. [9] In Fig. 2, we also present inverse ac susceptibility. In the temperature range 150 - 300 K, we have used a linear fit to our inverse susceptibility data. This linear fit, when extrapolated down

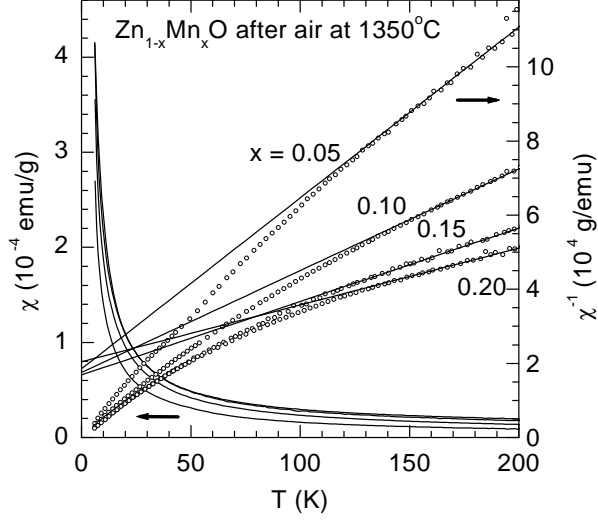


FIG. 2: ac susceptibility (curved continuous lines) and inverse ac susceptibility (open symbols) for $\text{Zn}_{1-x}\text{Mn}_x\text{O}$ samples synthesized in air. Straight lines present results of the linear fit to the temperature dependence of the inverse susceptibility.

to lower temperatures, intersects the $\chi^{-1} = 0$ axis at a negative temperature. This result indicates the presence of antiferromagnetic interactions in the $\text{Zn}_{1-x}\text{Mn}_x\text{O}$ samples. At lower temperatures, inverse ac susceptibility curves toward a temperature close to zero. This points to development of additional antiferromagnetic interactions between next neighbor Mn ions, which may turn on at lower temperatures. Similar nonlinear behavior of inverse susceptibility at low temperatures was reported in other semimagnetic semiconductors containing Mn. [9]. The annealing in Ar or Ar/ H_2 mixture under atmospheric pressure does not significantly change the value of ac susceptibility.

We have analyzed ac susceptibility results within the framework of the diluted Heisenberg antiferromagnet theory of Spalek *et al.* [9] At higher temperatures, ac mass susceptibility can be described by the formula

$$\chi = \frac{C_0 x}{T - \Theta(x)}, \quad (1)$$

where C_0 is the Curie constant defined as

$$C_0 = \frac{N(g\mu_B)^2 S(S+1)}{3k_B\rho}, \quad (2)$$

N - the number of cations per unit volume, $S = 5/2$ - effective spin of Mn^{2+} ion, ρ - mass density (although the lattice parameters change slightly with substitution of Mn, here we use the density $\rho = 5.55 \text{ g/cm}^3$ of pure

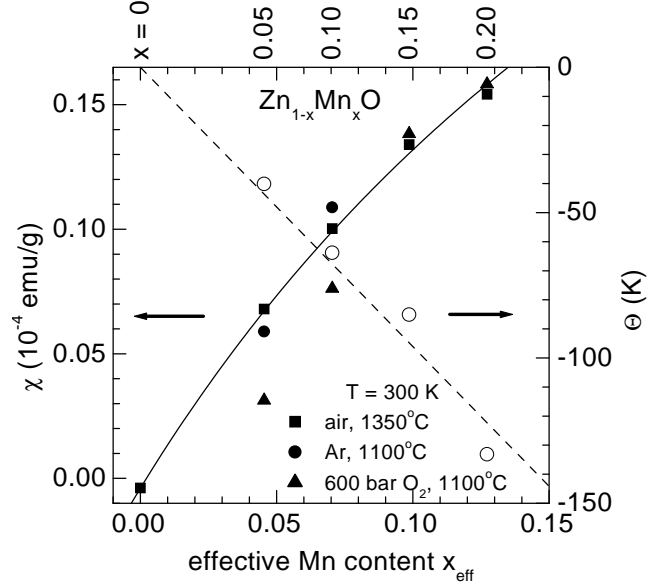


FIG. 3: Curie-Weiss temperatures Θ and ac susceptibility at $T = 300 \text{ K}$ for $\text{Zn}_{1-x}\text{Mn}_x\text{O}$ samples. The solid curve shows ac susceptibility calculated according to Eqs. (1) and (2), with $S = 5/2$ and derived $\Theta_0 = -961 \text{ K}$. The dashed line is a linear fit to the $\Theta(x_{eff})$ data. Nominal Mn content x is shown above the top axis.

ZnO), $\Theta(x) = \Theta_0 \cdot x$ - Curie-Weiss temperature. The Θ_0 constant is related to the exchange integral between the nearest Mn neighbors J_1 ,

$$\frac{2J_1}{k_B} = \frac{3\Theta_0}{zS(S+1)}, \quad (3)$$

where $z = 12$ is the number of nearest neighbors in the wurtzite structure of $\text{Zn}_{1-x}\text{Mn}_x\text{O}$.

ac susceptibility at $T = 300 \text{ K}$ for all studied samples is compiled in Fig. 3. First, pure ZnO is diamagnetic. Our measurements give us a value of ac susceptibility, which is 15-20% greater than the handbook value of $0.33 \cdot 10^{-6} \text{ emu/g}$. [10] This value does not change after argon annealing. The Mn-doped ZnO is paramagnetic. ac susceptibility increases with increasing Mn content x . Again, there is no significant influence of argon annealing on the ac susceptibility. High-pressure oxygen annealed samples show a decrease of room temperature susceptibility, especially large for small x . Subsequent annealing in air increases ac susceptibility to the initial values. The measured ac susceptibility is significantly lower than the theoretical expectation [Eqs. (1) and (2)] for a given nominal Mn content x . We suggest that due to disorder in our polycrystalline samples, not all Mn ions participate in superexchange interactions. Therefore, by putting C_0 from Eq. (2) and the measured χ and Θ into Eq. (1) we calculated the effective Mn content x_{eff} for

TABLE I: Comparison of material parameters determined from ac susceptibility for $\text{Zn}_{1-x}\text{Mn}_x\text{O}$ with other semimagnetic semiconductors containing Mn.

Material	Θ_0 (K)	C_M (emu K/mol)	$2J_1/k_B$ (K)	spin S	Source
$\text{Cd}_{1-x}\text{Mn}_x\text{Se}$	-743 ± 15	4.81 ± 0.1	21.2 ± 0.4	2.64 ± 0.06	Ref. [9]
$\text{Cd}_{1-x}\text{Mn}_x\text{Te}$	-470 ± 34	4.27 ± 0.17	13.8 ± 0.3	2.47 ± 0.05	Ref. [9]
$\text{Zn}_{1-x}\text{Mn}_x\text{O}$	-961 ± 49	4.07 ± 0.2	27.5 ± 1.4	2.5	This work
$\text{Zn}_{0.64}\text{Mn}_{0.36}\text{O}$	-1900	7.6	30	3.4	Ref. [7]

each nominal Mn content x . In Fig. 3, we present the values of the Curie-Weiss temperatures, obtained from the linear fit to the inverse susceptibility data for the air-annealed samples. From the linear dependence of Θ vs. x_{eff} , and assuming that $\Theta(x_{eff} = 0) = 0$, we derived the value of the exchange parameter $\Theta_0 = -961 \pm 49$ K. This value is close to previously reported values of Θ_0 for other semimagnetic semiconductors, but is much less than $\Theta_0 = -1900$ K, determined by Fukumura *et al.* [7]. The solid line in Fig. 3 represents the ac susceptibility dependence on x_{eff} , according to Eq. (1), using the our derived value of Θ_0 . Better agreement between the values of nominal x and effective x_{eff} should be obtained for single crystals of these materials, but crystal growth of $\text{Zn}_{1-x}\text{Mn}_x\text{O}$ with $x \geq 0.01$ from flux is difficult.[11]

In Table I we compare the results determined from ac susceptibility for our samples with those for several semimagnetic semiconductors. Taking Mn^{2+} spin $S = 5/2$, our values of Θ_0 and $2J_1/k_B$ are similar to other Mn-containing semiconductors. This supports the observation of the dominating role of superexchange in our materials.

The influence of high-pressure oxygen annealing on ac susceptibility is presented in Fig. 4 for our $\text{Zn}_{1-x}\text{Mn}_x\text{O}$ samples. Magnetic properties are dramatically changed after the annealing. For almost all $\text{Zn}_{1-x}\text{Mn}_x\text{O}$ samples, we observe a cusp in the temperature dependence of ac susceptibility [Fig. 4(a)], which indicates a transition to the spin-glass state. The freezing temperature of the spin-glass is equal to 11 - 16 K, depending on the manganese content. This value is consistent with $T_f = 13$ K, noted by Fukumura *et al.* [7] for a $\text{Zn}_{0.64}\text{Mn}_{0.36}\text{O}$ thin film. For high-pressure oxygen-annealed samples with $x = 0.10$, inverse ac susceptibility is now linear down to T_f [Fig. 4(b)]. The extrapolation of $\chi^{-1}(T)$ for this sample gives negative Curie-Weiss temperature Θ , which is close to T_f . Samples with $x = 0.15$ and $x = 0.20$ show unchanged values of Θ . Θ is radically changed for $x = 0.05$, becoming positive, which indicates the presence of ferromagnetic interactions in this material.

We can correlate the observed spin-glass behavior with the presence of ZnMnO_3 inclusions in our samples, detected by X-ray diffraction. The sample with $x = 0.15$ has the least amount of ZnMnO_3 . At the same time, no clear cusp in ac susceptibility is observed for this sample; only a change of slope at T_f can be seen. The presence of ZnMnO_3 impurity can be suppressed by subse-

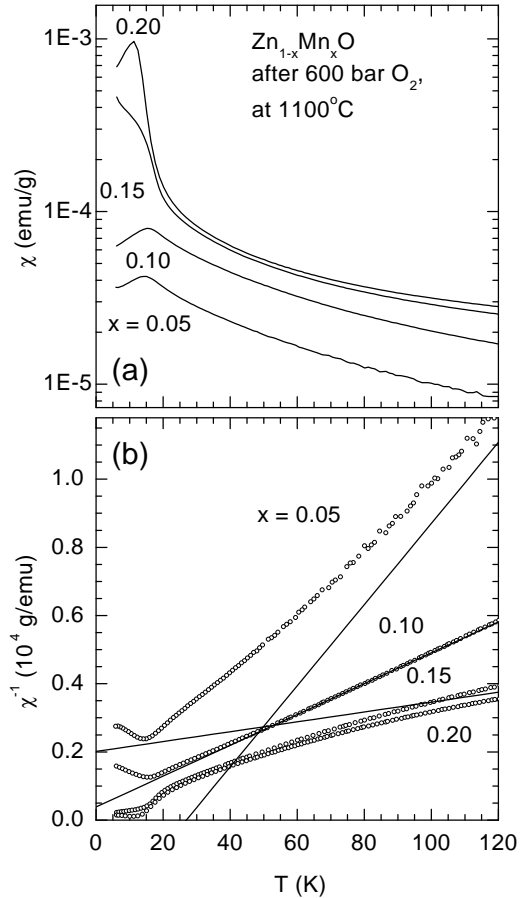


FIG. 4: (a) - ac susceptibility and (b) - inverse ac susceptibility for $\text{Zn}_{1-x}\text{Mn}_x\text{O}$ samples after high-pressure oxygen annealing.

quent annealing in air. The paramagnetic character of $\text{Zn}_{1-x}\text{Mn}_x\text{O}$ samples is restored after this annealing in air.

In Fig. 5, we present ac susceptibility for a $\text{Zn}_{0.9}\text{Mn}_{0.1}\text{O}$ sample measured at several frequencies in an ac magnetic field of constant amplitude $H_{ac} = 14$ Oe. One can observe a decrease of ac susceptibility be-

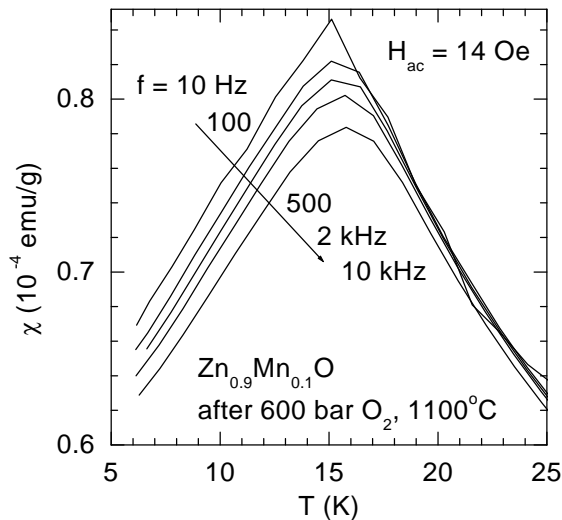


FIG. 5: Temperature dependence of ac susceptibility for $\text{Zn}_{0.9}\text{Mn}_{0.1}\text{O}$ sample at several frequencies.

low T_f with increasing frequency, and a shift of T_f towards higher temperatures. This observation confirms that the observed cusp in ac susceptibility is related to spin-glass behavior. [12] In dc magnetization, presented in Fig. 6, we can observe a difference between “Zero-field-cooled” (ZFC) and “field-cooled” (FC) magnetization, after cooling in a zero magnetic field measured on warming and on cooling in the magnetic field, respectively. Thermoremanent magnetization can be observed after field cooling to a temperature below T_f and switching off the magnetic field. Thermoremanent magnetization exhibits slow decay in time, which is presented in the inset to Fig. 6. All these phenomena are characteristic for spin-glass behavior.

One has to stress that the observed spin-glass behavior in our samples is different than in other diluted magnetic II - IV semiconductors. The main difference is that in other diluted magnetic semiconductors T_f scales with the manganese content as $\ln T_f \sim \frac{2}{3} \ln x$ or $\ln T_f \sim \alpha x^{-1/3}$. [13] For our high-pressure annealed samples, T_f is relatively independent of x . For example, T_f for other

Mn-substituted semiconductors with $x = 0.2$ is usually found in the range 4 to 10 K. [13] Our air-synthesized $\text{Zn}_{0.8}\text{Mn}_{0.2}\text{O}$ does not show spin-glass behavior down to $T = 2.6$ K. This observation again indicates the extrinsic nature of spin-glass behavior for high-pressure annealed samples.

In summary, we have studied magnetic properties of Mn-doped polycrystalline ZnO samples. Stoichiometric samples demonstrate Curie-Weiss behavior at higher temperatures, with mostly antiferromagnetic interac-

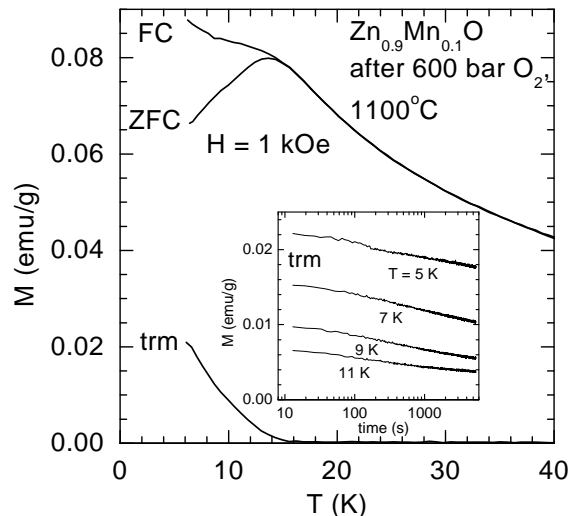


FIG. 6: “Zero-field-cooled” (ZFC), “field-cooled” (FC), and thermoremanent magnetization (trm) for $\text{Zn}_{0.9}\text{Mn}_{0.1}\text{O}$ sample. Inset shows time dependence of thermoremanent magnetization at several temperatures.

tions. Material parameters, determined from the ac susceptibility data show similarities between $\text{Zn}_{1-x}\text{Mn}_x\text{O}$ and other semimagnetic semiconductors substituted with Mn. High-pressure oxygen annealing induces spin-glass like behavior in $\text{Zn}_{1-x}\text{Mn}_x\text{O}$ by precipitation of ZnMnO_3 in the paramagnetic matrix.

This work was supported by the DARPA/ONR and the State of Illinois under HECA. The authors would like to thank Dr. Tomasz Dietl for valuable comments.

-
- [1] T. Dietl, H. Ohno, F. Matsukura, J. Cibert, and D. Ferrand, *Science* **287**, 1019 (2000).
 [2] K. Sato and H. Katayama-Yoshida, *Jpn. J. Appl. Phys.* **39**, L555, (2000).
 [3] K. Sato and H. Katayama-Yoshida, *Jpn. J. Appl. Phys.* **40**, L334, (2000).

- [4] K. Minegishi, Y. Koiwai, Y. Kikuchi, K. Yano, M. Kasuga, and A. Shimizu, *Jpn. J. Appl. Phys.* **36**, L1453, (1997).
 [5] T. Yamamoto et al., *Jpn. J. Appl. Phys.* **38**, L166, (1999).
 [6] M. Joseph, H. Tabata, and T. Kawai, *Jpn. J. Appl. Phys.*

- 38**, L1205, (1999).
- [7] T. Fukumura, Z. Jin, M. Kawasaki, T. Shono, T. Hasegawa, S. Koshihara, and H. Koinuma, *Appl. Phys. Lett.* **78**, 958 (2001).
- [8] K. Ueda, H. Tabata, and T. Kawai, *Appl. Phys. Lett.* **79**, 988 (2001).
- [9] J. Spałek, A. Lewicki, Z. Tarnawski, J. K. Furdyna, R. R. Galazka, and Z. Obuszko, *Phys. Rev. B* **33**, 3407 (1986).
- [10] *CRC Handbook of Chemistry and Physics, 80th Edition* 1999-2000, p. 4-136.
- [11] N. Ohashi, Y. Terada, T. Ohgaki, S. Tanaka, T. Tsurumi, O. Fukunaga, H. Haneda, and J. Tanaka, *Jpn. J. Appl. Phys.* **38**, 5028, (1999).
- [12] J. A. Mydosh, *Spin Glasses: an Experimental Introduction*, Taylor & Francis, London, Washington, DC 1993, and references therein.
- [13] A. Twardowski, H. J. M. Swagten, W. J. M. de Jonge, and M. Demianiuk, *Phys. Rev. B* **36**, 7013 (1987).